(This is a sample cover image for this issue. The actual cover is not yet available at this time.)

Earth and Planetary Science Letters 341–344 (2012) 48–57

Contents lists available at SciVerse ScienceDirect

Earth and Planetary Science Letters

journal homepage: www.elsevier.com/locate/epsl

Letters

Magma ocean influence on early atmosphere mass and composition

Marc M. Hirschmann

Department of Earth Sciences, University of Minnesota, Minneapolis, MN 55455, USA

ARTICLE INFO

Article history:
Received 11 February 2012
Received in revised form
5 June 2012
Accepted 7 June 2012
Editor: B. Marty

Keywords:
magma ocean
earth's early atmosphere
oxygen fugacity
deep carbon cycle

ABSTRACT

Redox conditions in magma oceans (MOs) have a key influence on the mass and composition of Earth's early atmosphere. If the shallow part of the MO is oxidized, it may be overlain by an H_2O–CO_2 atmosphere, but if the near-surface magma is close to equilibrium with Fe-rich alloy, then the atmosphere will consist chiefly of H_2, H_2O, and CO, and on cooling will be rich in CH_4. Although MOs are intimately associated with core-forming metal, the redox conditions in their shallow parts are not necessarily reducing. The magmatic Fe^{3+}/Fe^T ratio is set by equilibrium with metal at depth and homogenized through the magma column by convection. Indirect evidence suggests that the Fe^{3+}/Fe^T ratio of magmas in equilibrium with alloy at high pressure is greater than at low pressure, such that the shallow part of the MO may be comparatively oxidized and coexist with an atmosphere consisting chiefly of H_2O and CO_2. The mass of the atmosphere is dictated by the concentrations of volatile-species dissolved in the magma, which in turn are determined by partitioning between magma and alloy. Very strong partitioning of C into alloy may capture most of the carbon delivered to the growing planet, leaving behind a C-poor bulk silicate Earth (BSE) and a C-poor atmosphere. However, modest solubility of CH_4 in the magma may allow the BSE to retain significant C. Alternatively, if partitioning of C into alloy is extreme but the fraction of metal equilibrated with the MO is small, the alloy may become saturated with diamond. Floatation of diamond in the MO may retain a substantial inventory of C in the early mantle. BSE C may also have been replenished in a late veneer. Following segregation of metal to the core, crystallization of the MO may have prompted precipitation of C-rich phases (graphite, diamond, carbide), limiting the C in the early atmosphere and creating a substantial interior C inventory that may account for the large fraction of BSE carbon in the mantle today. Such precipitation could have occurred owing to a combination of the redox evolution of the crystallizing MO and cooling.

1. Introduction

The composition of Earth's primitive atmosphere has been a matter of debate for more than half a century. Miller and Urey (1959) assumed that Earth's early atmosphere consisted chiefly of NH_3, CH_4, H_2, and H_2O and famously showed that these reduced gases were conducive to prebiotic chemistry. In contrast, Rubey (1951) reasoned that an oxidized H_2O+CO_2 primitive atmosphere originated by volcanic degassing. Comparatively oxidized atmospheres dominated by H_2O, CO_2 and N_2 are less amenable to prebiotic chemosynthesis (Stribling and Miller, 1987; Bada, 2004). Exhalations of these more oxidized volcanogenic gases commenced at least as far back as 3.9 Ga (Delano, 2001) and possibly as early as 4.4 Ga (Trail et al., 2011). Ahrens et al. (1989) argued that an early H_2O+CO_2 atmosphere was delivered by comets. More recently, there has been increased emphasis on impact degassing of accreting chondritic material (Schaefer and Fegley, 2007; Hashimoto et al., 2007), which produces reduced gases (CH_4, H_2, H_2O, NH_3) more similar to those originally considered by Miller and Urey (1959).

The mass and composition of the early atmosphere has important influences on terrestrial evolution. As compared to storage in the interior, development of a massive atmosphere allows for significant volatile loss owing to large and small impacts (Melosh and Vickery, 1989; Genda and Abe, 2005) and, depending on the abundance of hydrogen, the potential of geochemical fractionation associated with hydrodynamic escape (Pepin, 1991). A thick atmosphere insulates the planet, greatly prolonging the persistence of magma oceans (MOs) (Abe and Matsui, 1985), affecting subsequent thermal evolution as the planet approaches equable conditions (Elkins-Tanton, 2008), and modulating succeeding climates and development of liquid water oceans (Zahnle et al., 2007). Finally, the early distribution of volatiles in the Earth represents the initial conditions for eventual development of modern deep H_2O and C cycles (Hirschmann, 2006; Dasgupta and Hirschmann, 2010).

Central to evolution of Earth's early atmosphere was development of one or more MOs, which resulted from the energy released by accretion, core formation, and impacts (Flaser and

E-mail address: mmh@umn.edu

0012-821X/$ - see front matter © 2012 Elsevier B.V. All rights reserved.
http://dx.doi.org/10.1016/j.epsl.2012.06.015

Birch, 1973; Davies, 1985; Benz and Cameron, 1990). The association of MOs with core formation and the high solubility of H and C in alloy may isolate much of the Earth's volatile inventory in the core (Fukai, 1984; Kuramoto and Matsui, 1996). Owing to the low solubility of H_2O and especially CO_2 in magma, thick atmospheres may develop (Abe and Matsui, 1985), containing much of the H_2O and virtually all of the carbon not removed to the core (e.g., Kuramoto and Matsui, 1996; Elkins-Tanton, 2008). The early mantle could therefore be comparatively volatile-depleted.

The possible massive atmosphere following MO crystallization contrasts with the distribution of volatiles prevailing today. For example, Elkins-Tanton (2008) calculated that 3–22% of the CO_2 and 5–30% of the H_2O in the bulk silicate Earth (BSE) would remain in the mantle following crystallization of a whole-mantle MO. In contrast, in the modern Earth, 50–95% of the BSE carbon is in the mantle (Sleep and Zahnle, 2001; Dasgupta and Hirschmann, 2010). This large deep reservoir is a key feature of the modern carbon cycle, allowing volcanogenic CO_2 to modulate climate on a range of time scales, from termination of snowball Earth conditions (Hoffman et al., 1998) to acceleration of Pleistocene deglaciations (Huybers and Langmuir, 2009). The modern distribution of BSE H_2O, 17–70% of which is in the mantle (Hirschmann, 2006), is more similar to these putative initial conditions. The difference between initial conditions is therefore most pronounced for C: degassing of a MO is thought to produce an exosphere with a low H/C ratio compared to the mantle, whereas at present the opposite is true (Hirschmann and Dasgupta, 2009).

A key consideration is that chemical interactions with a MO can have profound influence on the composition and mass of the overlying atmosphere. Regardless of whether the gases delivered to the surface were originally oxidized or reduced, the very large redox capacity of the MO with which it coexists will likely determine the atmosphere's oxidation state, and hence the abundances of C–O–H (CO_2, CH_4, CO, H_2O, H_2) species. The atmosphere may also be affected by precipitation of graphite, diamond, or carbide or equilibration with alloy (Fukai, 1984; Kuramoto and Matsui, 1996), which can limit vapor pressures in the magma and therefore, atmospheric mass.

A critical but previously unrecognized feature of the chemical structure of MOs is that oxygen fugacity, f_{O_2}, should vary with depth. In this paper, the zonation of f_{O_2} in MOs is considered and the possible consequences for volatiles in MOs and overlying atmospheres are explored.

2. Magma ocean–atmosphere equilibration

Chemical equilibration between a MO and its overlying atmosphere should be efficient unless an impermeable lid develops. The duration of MO crystallization ($\sim 10^4$–10^7 yr; Abe and Matsui, 1985; Zahnle et al., 2007; Elkins-Tanton, 2008) is long compared to the likely time required to approach chemical equilibrium with the overlying atmosphere. For comparison, the time required for modern (H_2O) oceans and atmosphere to equilibrate pCO_2 is $\sim 10^2$ yr (Archer et al., 2009), but time scales should be briefer for MOs, owing to vigorous convection in both reservoirs, with convective mixing times in a 3000 km magma ocean being a matter of weeks (e.g., Solomatov, 2000), and to >2000 K temperatures at the magma–vapor interface (e.g., Abe and Matsui, 1985).

Oxygen fugacity affects critically the chemistry of a C–H–O atmosphere (Fig. 1). Under oxidizing conditions, the chief species are H_2O and CO_2, but under reducing conditions, CO and H_2 predominate. On cooling, these react to form CH_4, leaving an atmosphere rich in H_2, CH_4, and H_2O. One may at first expect atmospheres overlying MOs to be reduced, as MOs are associated

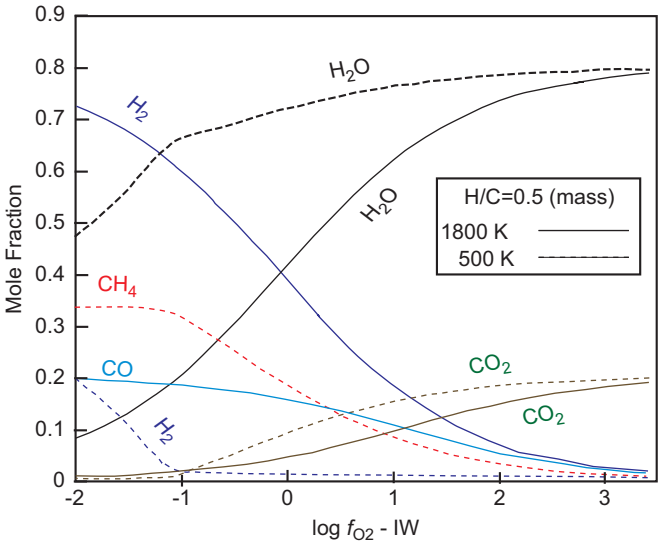

Fig. 1. Calculated mole fractions of molecular species for a gas with a mass H/C ratio of 0.5. The calculation at 1800 K (solid curves) is performed as function of f_{O_2}, where f_{O_2} is calculated relative to that defined by the coexistence of iron and wüstite (IW) (O'Neill, 1988). Under oxidizing conditions the chief gas species are H_2O and CO_2, and under reduced conditions they are H_2, CO, and H_2O. Cooling of this gas to 500 K (dashed lines) produces reduced gases that are chiefly H_2O, CH_4, and H_2. Note that the f_{O_2} scale applies only to the 1800 K calculation; the 500 K calculation is produced simply by cooling the 1800 K gas. Gas species computed at 100 kPa confining pressure using the calculation of Kress (2004).

with core formation and hence equilibration with metal. For the late stages of Earth's accretion, when the mantle approached its current FeO content of 8 wt%, such conditions are $\sim 1.5 \pm 0.5$ log units below that buffered by the coexistence of pure iron and wüstite (IW) (Frost et al., 2008). This would seem to invalidate models in which MOs are overlain by H_2O–CO_2 atmospheres (e.g., Zahnle et al., 2007; Elkins-Tanton, 2008). However, here I will show that the oxidation state at the top of a MO depends on the depth of magma–metal equilibration and that, for likely properties of Fe in magma at high pressure, H_2O–CO_2 atmospheres may indeed overlie MOs in which metal is present at depth or from which metal has already segregated to the core.

3. Oxygen fugacity zonation in a magma ocean

I assume that metal-silicate equilibrium in a MO is established at depth. This depth may correspond to the top of a "metal pond" at the base of the MO (Stevenson, 1990) or to a mean depth of equilibration established through a combination of processes, including episodes of Fe-rich metal droplets passing through the magma column (Rubie et al., 2003). Estimates of the mean depth of equilibration range from 25 to 60 GPa (Li and Agee, 1996; Chabot et al., 2005; Corgne et al., 2008; Kegler et al., 2008).

During accretion events, metal passing through the MO column can react with the MO, enforcing metal saturation at all depth, and imposing Fe^{3+}/Fe^T ratios that vary with pressure accordingly. However, these events are brief, as simulations have found that metal rain-out is efficient for the full spectrum of expected metal droplet sizes (Höink et al., 2007; Ichikawa et al., 2010), and the column should become metal free in ~ 2 weeks (Ziethe, 2009). Vigorous convection returns the MO to the condition of homogeneous Fe^{3+}/Fe^T with a value set by the mean depth of equilibration of 25–60 GPa. Consequently, in the rest of this work, I assume that the vertical column of the MO is metal-free except perhaps at its base with the Fe^{3+}/Fe^T ratio set by deep

equilibration with molten alloy or, if metal is absent, at a higher value.

Although the f_{O_2} at the depth of magma–metal equilibration will be near IW−1.5, this will not define the f_{O_2} throughout the magma column. Rather, f_{O_2} will vary with depth owing to the different molar volumes of Fe^{2+} and Fe^{3+} in melts (e.g., Kress and Carmichael, 1991), as can be seen from the reaction:

$$\underset{\text{magma}}{\text{FeO}} + \frac{1}{4}O_2 \Leftrightarrow \underset{\text{magma}}{\text{FeO}_{1.5}} \quad (1)$$

which depends on pressure (Kress and Carmichael, 1991; O'Neill et al., 2006):

$$\log f_{O_2} = \frac{4}{2.303}\left(\Delta\overline{G}^0 + \int_1^P \Delta\overline{V}\,dP + RT\ln\frac{X_{FeO_{1.5}}^{melt}\gamma_{FeO_{1.5}}^{melt}}{X_{FeO}^{melt}\gamma_{FeO}^{melt}}\right) \quad (2)$$

here $\Delta\overline{G}^0$ is the standard state change in free energy of reaction (1), $\Delta\overline{V}$ the difference in the partial molar volumes of the ferric and ferrous oxide components in the melt, and X_i^{melt} and γ_i^{melt} are the mole fractions and activity coefficients of each component. Eq. (2) shows that f_{O_2} will vary with pressure according to the magnitude of $\Delta\overline{V}$. Importantly, a relation analogous to Eq. (2) can be written for the IW reaction and if the values of $\Delta\overline{V}$ for each reaction are not equal, then relative to the IW buffer, f_{O_2} at fixed magma Fe^{3+}/Fe^T varies with depth and therefore so will Fe^{3+}/Fe^T at metal saturation (∼IW−1.5).

Low pressure determinations of the partial molar volumes and compressibilities of Fe_2O_3 and FeO in silicate melts (Lange and Carmichael, 1987; Kress and Carmichael, 1991), as well as Mössbauer determinations of Fe^{3+}/Fe^{2+} speciation from glasses quenched from 0 to 4 GPa (Mysen and Virgo, 1985; O'Neill et al., 2006), indicate that decompression at constant Fe^{3+}/Fe^T causes silicate melts to become more reduced relative to metal-oxide buffers (Fig. 2). This is because the low pressure partial molar volume of $FeO_{1.5}$ in silicate melts is large compared to that of FeO (Kress and Carmichael, 1991).

If the trend evident in Fig. 2 were to apply throughout the pressure range of a MO, then well mixed magmas in equilibrium with metal at depth would be yet more reduced at lower pressure (Fig. 3), and the atmosphere above such MOs would be dominated by H_2 (Fig. 1). It would also lead to some interesting dynamics, as shallow regions would precipitate Fe, becoming FeO-depleted and perhaps producing a gravity-stratified MO. However there are reasons to suspect that this trend reverses at higher pressure, such that melts of the same Fe^{3+}/Fe^T become more reduced relative to IW with increasing pressure. If so, then MOs could be comparatively oxidized in their shallow reaches. The reasons are as follows:

(1) The low pressure trend for silicate melt is opposite to that for solid peridotite, for which isochemical self-compression above 3 GPa leads to reduced conditions relative to IW (Fig. 3). This is because Fe^{3+} is stabilized in the high-coordination environments provided by deep mantle minerals, such as the octahedral sites in garnet (O'Neill et al., 1993; McCammon, 1997; Frost and McCammon, 2008). Pressure also stabilizes high cation coordination in silicate liquids resembling those found in minerals (e.g., Ghiorso, 2004; Stixrude and Karki, 2005) and so analogous stabilization of Fe^{3+} in melts seems likely at high pressure.

(2) In silicate melts, the partial molar volume of VI-coordinated Fe^{3+} is 25% smaller than that of IV-coordinated Fe^{3+} (Liu and Lange, 2006), and so at high pressures, highly coordinated Fe^{3+} becomes more stable and $\Delta\overline{V}$ in Eq. (2) diminishes. Mössbauer spectroscopy of quenched Na_2O–FeO^T–SiO_2 glasses suggests shifts from IV to VI coordinated Fe^{3+} near 3–4 GPa (Mysen and Virgo, 1985; Brearly, 1990), though quantification is poor. It is also true that Fe^{2+} takes on higher coordination states with increased pressure, but this effect is likely smaller than that for Fe^{3+}, as at low pressure the FeO component in silicate melts has a much more compact structure than that of Fe_2O_3. For example, using the partial molar volumes of Ghiorso and Kress (2004), the ionic porosity

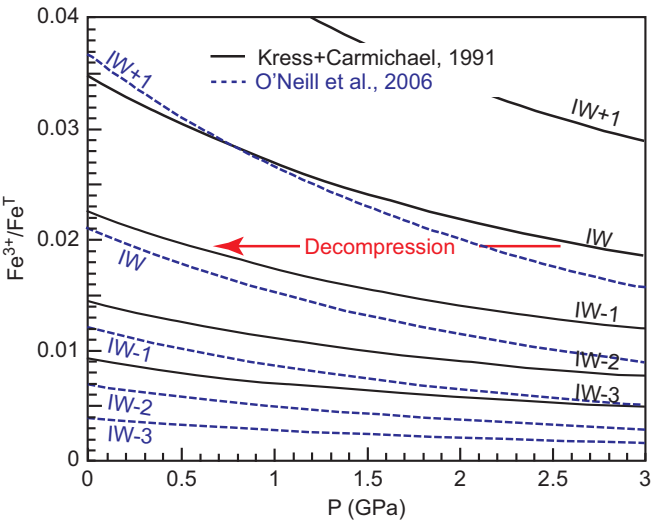

Fig. 2. Fe^{3+}/Fe^T of silicate melts as a function of pressure at oxygen fugacities fixed relative to the iron–wüstite (IW) buffer (calculated from O'Neill (1988), with the equation of state of Campbell et al. (2009)). Trends are calculated from the models of Kress and Carmichael (1991) (their Eq. 7) and O'Neill et al. (2006). As illustrated by the red arrow, decompression at fixed values of Fe^{3+}/Fe^T leads to reduction relative to the IW buffer. Quantitative differences between the models are likely because of small amount of Fe^{3+} present at these reducing conditions and because both are extrapolated from data obtained under more oxidizing conditions. (For interpretation of the references to color in this figure legend, the reader is referred to the web version of this article.)

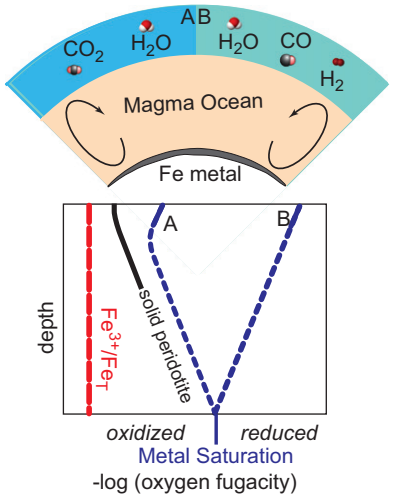

Fig. 3. The Fe^{3+}/Fe^T at the base of a MO will be that set by metal-silicate equilibrium. The vertical gradient in f_{O_2} will be determined by the influence of pressure at fixed Fe^{3+}/Fe^T, assuming the latter is homogenized by vigorous convection. If decompression produces more oxidized conditions relative to IW (A), as is the case for solid peridotite (shown schematically, after Frost and McCammon (2008)), then the shallow portions of the MO will be in equilibrium with an H_2O–CO_2 atmosphere. If decompression produces more reduced conditions (B), then the shallow MO will coexist with an H_2–H_2O–CO atmosphere. The effect of pressure on the redox state of magma at fixed Fe^{3+}/Fe^T is known only at 3 GPa (O'Neill et al., 2006) (solid portion of blue trends). If that trend continues to high pressure, then case B will prevail. If that trend reverses at high pressure and becomes similar to that of solid peridotite, then case A applies. (For interpretation of the references to color in this figure legend, the reader is referred to the web version of this article.)

(Carroll and Stolper, 1993) of the FeO component is 43%, whereas that of Fe_2O_3 is 51%.

For these reasons, in the remainder of the paper, I assume that Fe^{3+} is stabilized at high pressure and that deep MOs are more oxidized near the surface than at depth. Whether this is true can only be determined by new experiments, but it is certain that there should be a vertical zonation in MO redox state relative to IW unless the differences in volumes between Fe^{2+} and Fe^{3+} in silicate liquids are exactly the same as the differences between Fe and Fe^{2+} in solid Fe metal and wüstite. If this assumption is in error, future work should explore the consequences of the opposite redox zonation for volatile evolution in early terrestrial planets.

If Fe^{3+} is stabilized in melts at high pressure, an important question is the pressure above which silicate liquids become more reduced with increasing depth. Experimental investigations are needed, but the reversal could be as shallow as 150–200 km. First, the trend of reduction with increasing depth in solid peridotite begins near 3 GPa, at the onset of garnet stability, and the pressures at which coordination changes in silicate liquids occur are commonly similar to those at which analogous polymorphic transitions occur in minerals (Ghiorso, 2004; Stixrude and Karki, 2005). Second, octahedral coordination of Fe^{3+} has been inferred in alkali iron silicate melts at 3–4 GPa based on Mössbauer spectroscopy (Mysen and Virgo, 1985; Brearly, 1990), a pressure similar to that for which increased coordination of the other principle trivalent cation in melt, Al^{3+}, is manifested (Ghiorso, 2004; Allwardt et al., 2005). This is much lower than the mean pressure of metal-silicate equilibration in the MO (e.g., 25–60 GPa) and so it is plausible that the mean Fe^{3+}/Fe^{T} of the MO was high (Fig. 3). For comparison it is instructive to recall that Mg-perovskite in equilibrium with Fe at 25 GPa has ~50% Fe^{3+}/Fe^{T} (McCammon, 1997). Thus, for magma–metal equilibration in the terrestrial MO, convective mixing may produce comparatively oxidized conditions at shallow depths.

Magmatic vapor that, on cooling, is dominated by H_2O and CO_2 is stabilized for oxygen fugacities above ~IW+0.5 (Fig. 1). Such a comparatively oxidized atmosphere could be produced by low pressure, high temperature equilibration with a magma that has a relatively small Fe^{3+}/Fe^{T} ratio: 0.025 and 0.05 at 2000 °C and 0.1 MPa, based on O'Neill et al. (2006) and Kress and Carmichael (1991), respectively.

4. Dissolved volatiles in a MO with an f_{O_2} gradient

If the shallow reaches of a MO are comparatively oxidized such that the overlying atmosphere consists chiefly of H_2O and CO_2, then the dissolved volatile content can be calculated from simple solubility laws (Pan et al., 1991; Moore et al., 1998). For example, for CO_2 and H_2O partial pressures of 30 MPa (e.g., Zahnle et al., 2007), the underlying MO will have 1.2 wt% H_2O and 180 ppm CO_2 (Fig. 4). The large differences in solubility mean that most of the growing planet's H_2O is dissolved in the MO, but that most of the CO_2 is in the atmosphere: for a MO equal to the mass of the present-day upper mantle, 90% of the H_2O and 10% of the CO_2 will be dissolved in the MO. For a whole-mantle MO, these numbers rise to 99% and 30%.

Importantly, the C–O–H volatiles dissolved in the shallow MO may become oversaturated with volatile-rich solids at depth and/or may be partitioned into molten alloy, if present. Extrapolation of the 7.5 GPa H partitioning experiments of Okuchi (1997) to temperatures (1800–2500 °C) relevant to MOs suggests an alloy/silicate partition coefficient, $D_H^{all/sil}$, of 5–10. Thus, if the MO

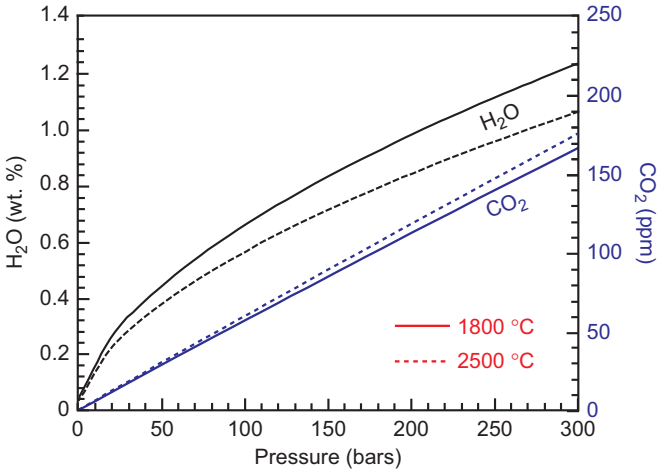

Fig. 4. Solubility of H_2O and CO_2 in magma as a function of partial pressures. The solubilities in peridotitic magma are not known from experiment, and so, to a first approximation, those for basalt are taken from Pan et al. (1991) and Moore et al. (1998) for CO_2 and H_2O respectively.

interacts with appreciable metal, the silicate and vapor envelopes may lose much of their H_2O to the core.

Significant carbon also may be removed from the silicate magma and atmosphere, either by partitioning into available alloy or precipitation of graphite, diamond, or carbide. The dissolved CO_2 content of graphite/diamond-saturated silicate liquids increases with temperature and decreases with pressure and as conditions become more reduced (Holloway, 1998; Hirschmann and Withers, 2008). Calculated along a MO adiabat, C saturation requires lower dissolved CO_2 with increasing depth and diminishes by an order of magnitude for each log unit decrease in f_{O_2} (Fig. 5). For example, at 25 GPa, diamond saturation occurs at CO_2 concentrations between 7 (IW−2) and 70 ppm (IW−1). At the same pressure and f_{O_2} range, but the much cooler temperatures prevailing at the peridotite solidus, solubilities are less than 1 ppm. Depending on Fe activity and temperature, the saturating C-rich phase may be carbide and if so, the maximum dissolved CO_2 at a given T, P, and f_{O_2} could be less than illustrated in Fig. 5.

Experimental data determining partitioning of C between silicate liquid and molten alloy are available only for extreme conditions (very low f_{O_2}, high f_{H_2}, Kadik et al., 2011) not applicable to the later stages of Earth's accretion. However, combining the thermodynamics of solubility of C-saturated silicate liquid (Holloway et al., 1992; Holloway, 1998; Hirschmann and Withers, 2008) with experimental determinations of graphite saturation in Fe–C molten alloys (e.g., Dasgupta and Walker, 2008; Nakajima et al., 2009) allows calculations of partitioning for C partitioning between molten alloy and silicate liquid, as $D_C^{all/sil} = D_C^{all/graphite} D_C^{graphite/sil}$. Values of $D_C^{graphite/sil}$ can be derived from the saturation calculations illustrated in Fig. 5A; those for $D_C^{all/graphite}$ are relatively insensitive to intensive variables and are approximately 0.12–0.2 (Dasgupta and Walker, 2008; Nakajima et al., 2009), although smaller values are possible for S-rich melts (Zhimulev et al., 2012). Resulting values of $D_C^{all/sil}$ are large, as dissolved CO_2 becomes low (Fig. 5B). For example, metal-saturated magma along a MO adiabat at 25 GPa with 7–70 ppm CO_2 has corresponding values of $D_C^{all/sil} = 2\times10^5 - 2\times10^4$.

An important caveat for the calculations in the preceding paragraphs is that they assume that all C is dissolved as CO_3^{2-}. However, under reducing conditions, other C–O–H species, most notably CH_4, likely exceed dissolved carbonate. This will increase the dissolved C content of C-saturated magmas, making the

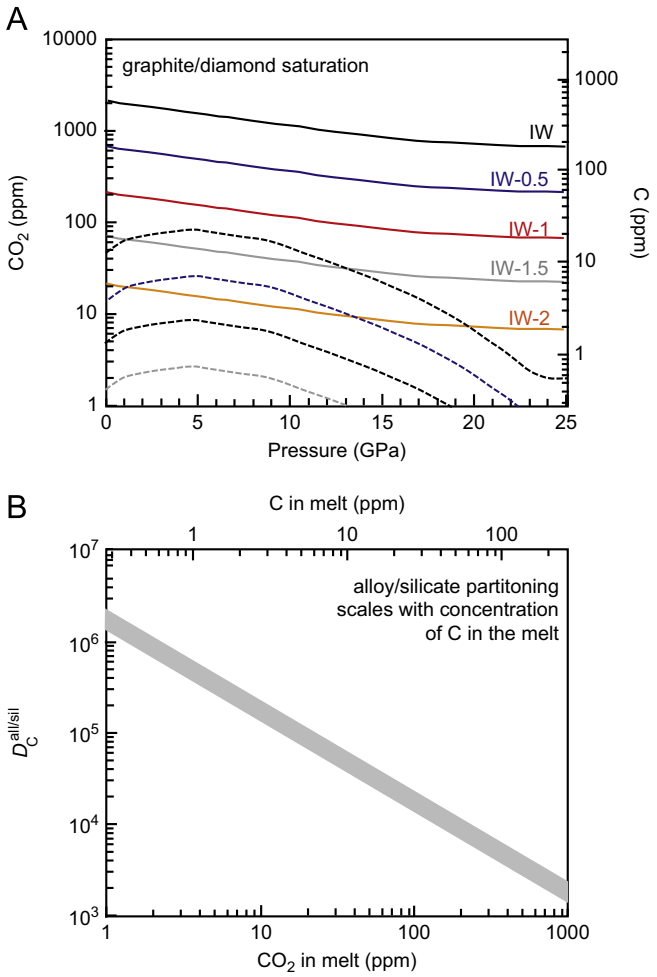

Fig. 5. (A) Calculated solubility of CO_2 or C for graphite- or diamond-saturated magmas. Solid curves are calculated along an adiabatic geotherm for a magma ocean that is above the liquidus to a pressure of 25 GPa (Stixrude et al., 2009). The dashed curves are calculated at temperatures and pressures of the dry peridotite solidus (Hirschmann, 2000; Hirschmann et al., 2009). Saturation calculations follow those of Holloway et al. (1992) and Hirschmann and Withers (2008), with adjustments for diamond stability using the graphite and diamond equations of state from Day (2012). Calculations assume that C is dissolved only as CO_3^{2-}. If appreciable CH_4 is dissolved, these are *minima*. Note that these calculations are incorporated into two different thermodynamic relationships—one relating graphite or diamond saturation to the ratio of CO_2 and O_2 fugacities and the second relating CO_2 fugacity to dissolved carbonate concentration. The first calculation is robust over the calculated pressure range, but the second is based on experimental measurements that are available only to 3 GPa. Extrapolation of this model to higher pressure involves some loss of accuracy, but most of the calculated variations in CO_2 concentrations derive from the first portion of the calculation. (B) For a given concentration of C or CO_2 dissolved in the magma at graphite/diamond saturation (i.e., $D_C^{all/graphite}$), the value of $D_C^{all/sil}$ can be estimated from known values of $D_C^{all/graphite}$. The gray band is derived from experimental values of $D_C^{all/graphite}$ and $D_C^{all/diamond}$ (=0.125–0.2; Dasgupta and Walker, 2008; Nakajima et al., 2009) which show that C-rich alloy saturates at 5–8 wt% C.

calculations under reduced conditions in Fig. 5A minima. It will decrease $D_C^{all/sil}$ proportionally (Fig. 5B). Experimental constraints on the solubility of CH_4 species in magmas remain sparse. Mysen et al. (2009) and Kadik et al. (2011) reported CH_4 solubilities of up to 0.5 wt% in Na-silicate and synthetic peralkaline rhyolite liquids, respectively, but Ardia et al. (2011) found no more than ~0.05 wt% in synthetic basalt. However, CH_4 concentrations are sensitive to H_2 fugacity, f_{H_2}, as f_{CH_4} is proportional to $(f_{H_2})^2$. All of these experiments were performed with high H_2 fugacities that may be greater than expected in plausible MOs. In the following discussions, a range of reasonable values of C saturation and $D_C^{all/sil}$ are considered.

5. Volatile processing in MOs

The distribution of volatiles between the core, mantle and atmosphere resulting from MO processes can be understood by considering two stages, metal-present and metal-absent. The former affects the inventory of H and C sequestered in the core, whereas the latter influences their distribution between the mantle and atmosphere following MO solidification. The transition may occur in the aftermath Moon-forming giant impact, which may have been the last time appreciable metal was present in the MO.

5.1. Metal-rich MO

It has long been recognized that the solubilities of H and C in core-forming alloy are large and that extensive interaction between core-forming metal, MOs, and overlying vapors can result in core sequestration of large fractions of the H and C in a growing planet (Fukai, 1984; Kuramoto and Matsui, 1996). It is common to assume that the partitioning of H and C involved equilibration of the entire mass of the core with the proto-mantle (e.g., Kuramoto and Matsui, 1996; Okuchi, 1997; Dasgupta and Walker, 2008; Nakajima et al., 2009). This leads to the conclusion that the core is highly enriched in H and C and that core formation left behind a volatile-depleted mantle. However, nearly all core-forming metal possibly avoided interaction with most of Earth's volatile inventory. Dahl and Stevenson (2010) concluded that ~10% of the core (mass equal to 5% of the mantle) equilibrated with the mantle, virtually all occurring during the early stages of accretion. As most volatiles accreted towards the end of Earth's assembly (e.g., Raymond et al., 2007), it seems that MO volatiles present during the later stages of accretion reacted with a small fraction of metal.

Combining H_2O and CO_2 solubilities in magma (Fig. 4) with silicate/metal partitioning of H (Okuchi, 1997) and C allows calculated volatile partitioning between a MO, overlying atmosphere, and coexisting metal (Fig. 6). The concentrations of H and C in metal are related to the partial pressures of H_2O and CO_2 in the atmosphere (Fig. 6A), as these fix the concentrations of H and C in silicate, which in turn determine the activities of H and C at depth. Notably, high values of $D_C^{all/sil}$ limit the possible density of the overlying atmosphere and concentration of CO_2 in the magma to <5 MPa, 30 ppm ($D_C^{all/sil}=10^4$) or <0.8 MPa, 3 ppm ($D_C^{all/sil}=10^5$). This is because the C concentration in alloy becomes sufficiently high (~8 wt%) to saturate in an additional C-rich phase (graphite, diamond, or carbide), thereby forcing any additional C beyond these concentrations into the co-saturating solid. In turn, back-reaction between the magma and the atmosphere prevents high partial pressures of CO_2. Thus, if large values of $D_C^{all/sil}$ prevail, much of the C available is extracted from the atmosphere and magma and resides in solids. On the other hand, if $D_C^{all/sil}$ is below 10^3 and the alloy/silicate ratio is small ($<1\%$), then much of the C remains in the atmosphere.

Even when the metal proportion is small, the fraction of H and particularly C stored in reduced phases (alloy, carbide, diamond) is significant (Fig. 6B). For large alloy/silicate ratios (5%), up to 40% of the total H may be in the metal, though more modest fractions (12–22%) are stored there for alloy/silicate ratios of 1–2%. In contrast, carbon is dominantly found in solids even if the alloy/silicate ratio is as little as 1% and $D_C^{all/sil}=10^3$, and if $D_C^{all/sil}$ is significantly greater than 10^3, virtually all in solids for yet smaller alloy/silicate ratios. Note however, that under these circumstances (high $D_C^{all/sil}$, low alloy/silicate ratio) much of this carbon will be in diamond rather than in alloy.

For cases where $D_C^{all/sil}$ is large and C-rich alloy saturates with an additional C-rich phase, a key question is the identity and fate

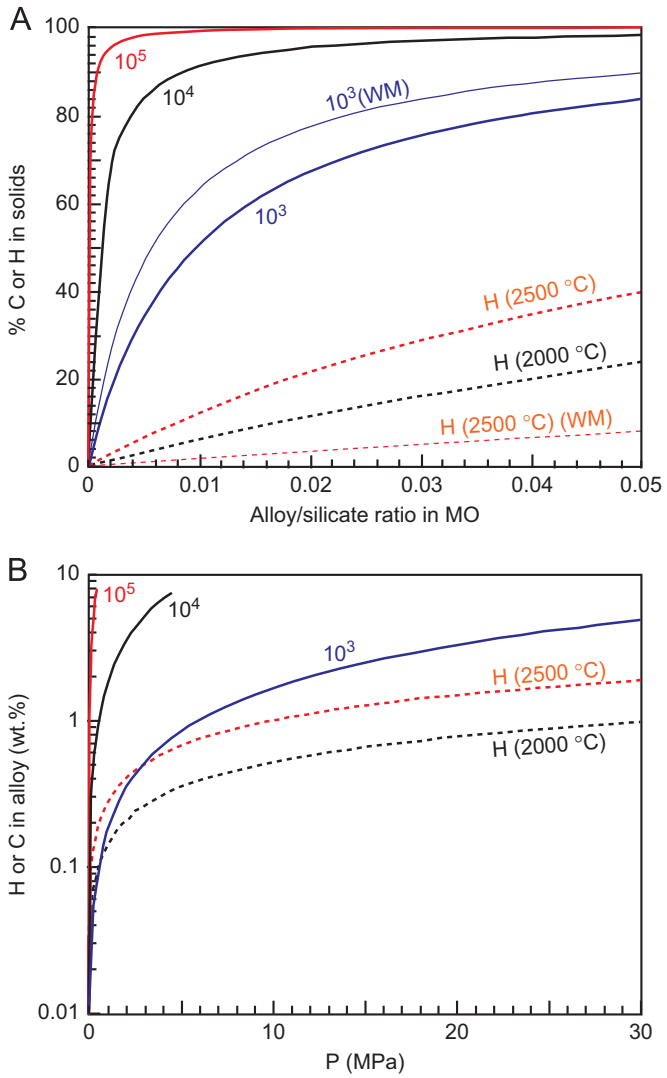

Fig. 6. (A) Mass proportion of H or C in solids (alloy, carbide, diamond, or graphite) compared to that in a MO and overlying atmosphere as a function of the metal/silicate mass ratio present in a MO. H mass balances are calculated using the alloy/silicate partition coefficients of Okuchi (1997), extrapolated to 2000 and 2500 °C. C mass balances are calculated using values of $D_C^{all/sil} = 10^3$, 10^4, and 10^5. Where noted ("WM") calculations are for whole-mantle MO, all others are for a MO restricted to the upper mantle. Because much of the H is dissolved in silicate, a smaller proportion of H is sequestered in metal in a whole mantle MO. Carbon is dominantly found in solids and in the atmosphere, and so, a larger MO at a given metal/silicate mass ratio also means a greater mass of metal relative to the atmosphere, and hence, an enhanced proportion of C in the alloy. (B) The concentration of H or C in alloy as a function of the partial pressure of H_2O or CO_2 in the atmosphere. The alloy is assumed to be saturated in C at 8 wt% C (e.g., Nakajima et al., 2009), which corresponds to CO_2 partial pressures of 8 and 50 MPa for $D_C^{all/sil} = 10^5$ and 10^4, respectively.

of that phase. Carbide could segregate to the core along with the molten alloy, but at high temperature (e.g., >1700 °C at 14.5 GPa, Nakajima et al., 2009), the co-saturating phase will be diamond. At pressures >20 GPa, diamond is less dense than ultramafic magma (Suzuki et al., 1995) and will not segregate to the core, but instead float to intermediate MO depths near 600 km and remain as a substantial fraction of the C ultimately stored in the solidified mantle (Fig. 7). For example, if $D_C^{all/sil} = 10^5$ and the alloy/silicate ratio in a whole-mantle MO is 0.01, then for an initial C mass of 4×10^{21} kg ($=4$–22 X modern BSE; Dasgupta and Hirschmann, 2010), 80% will go to the core, 0.8% in the molten mantle, 1.8% in the overlying atmosphere, and 17.4% ($=0.5-3.8$ X BSE) in diamond.

5.2. Evolution of metal-free MOs

Following segregation of the core, volatiles are present in the MO, perhaps largely as diamond, and in the overlying atmosphere. These inventories evolve as the MO crystallizes. When solidification is complete, some portion of the H_2O and C remain in the mantle and the rest is in the atmosphere. In this section, the focus is on the behavior of C. The evolution of H_2O inventories during MO crystallization, and the partitioning of H_2O between crystallizing nominally anhydrous minerals, magma, and vapor have been considered previously by Kawamoto et al. (1996) and Elkins-Tanton (2008).

I first focus on metal-free MOs that evolve from metal-present ones and consider MOs descended from a giant impact separately. For the first case, an H_2O–CO_2 atmosphere overlies a MO that is oxidized near its surface and progressively more reduced at depth, such that it is close to metal-saturated near its base (IW -1.5 ± 0.5). If partitioning of C into alloy is not severe (e.g., $D_C^{all/sil} = \sim 10^3$), a substantial fraction of the carbon remains in silicate and vapor and the atmospheric CO_2 partial pressure may be high; if the partitioning is extreme (10^5), virtually all the carbon is removed to the core or precipitated as diamond (Fig. 5B) and little CO_2 is in the overlying atmosphere. Either way, the low magmatic solubility of CO_2 dictates that the majority of C not removed to the core or stored as floating reefs of diamond will be in the overlying atmosphere. For a whole-mantle MO, 69% of the C not in solids will be in the atmosphere and for an upper mantle MO, 90% will be in the atmosphere.

The loss of metal from the MO leaves a magma that is close to saturation in alloy and potentially has an additional C-rich phase. If crystallization of Mg-perovskite with high intrinsic Fe^{3+}/Fe^T (McCammon, 1997) lowers the Fe^{3+}/Fe^T in the residual magma or forces disproportionation of magmatic Fe^{2+} (Wood et al., 2006), the system will be driven to metal and potentially diamond/carbide saturation, resulting in storage of C together with the crystallizing silicates. This may persist throughout crystallization of the lower mantle and perhaps the deeper parts of the upper mantle. At low pressures, Fe^{3+} becomes incompatible in crystallizing silicate, and remaining liquids may become oxidized.

Irrespective of the f_{O_2} evolution during MO crystallization, mere cooling may cause saturation in C-rich phases. The strong temperature dependence of the graphite/diamond-saturated concentration of CO_2 in silicate melts (Hirschmann and Withers, 2008) means that at constant f_{O_2} relative to IW, the CO_2 concentration for graphite/diamond saturation diminishes by nearly two orders of magnitude on cooling from a deep MO adiabat down to the peridotite solidus (Fig. 5). Although the temperature dependence of the solubility of CH_4 is not known, dissolved methane may inhibit C-phase precipitation and so the saturation curves in Fig. 5 are minima.

Precipitation of C-rich phases during MO crystallization buffers the dissolved C, thereby limiting C in the overlying atmosphere. If the saturation condition at the base of the MO evolves towards very low concentrations of dissolved C, as suggested by the low near-solidus saturation curves in Fig. 5, then the MO will become C-saturated, which will cause much of the CO_2 in the overlying atmosphere to dissolve into the magma. This produces a magma ocean carbon pump (Fig. 8), drawing down much of the atmospheric C and precipitating it along with the crystallizing silicates.

5.3. After the giant impact

The processing of volatiles in a MO that descends from a giant impact presents a special case. Very high temperatures vaporize much of the mantle (Canup, 2004), and devolatilize the remaining

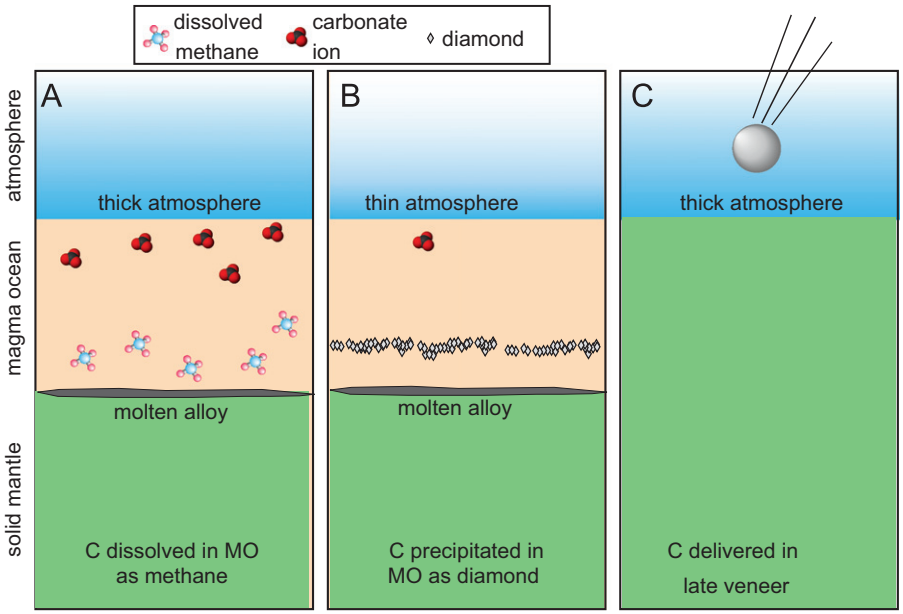

Fig. 7. Three scenarios that can account for the large C reservoir in the modern bulk silicate Earth (BSE). (A) Modest solubility of CH_4 or another reduced C-bearing species in the deep reduced portion of a MO inhibits sequestration of C in core-forming alloy. The high dissolved C is present as dissolved carbonate ion in the shallow oxidized MO region and supports a thick C-rich overlying atmosphere. (B) The solubility of reduced C deep in the MO is low owing to extreme partitioning into alloy, but the mass of available alloy is small. Diamond precipitates owing to saturation of C-rich alloy. Less carbonate is present in the shallow MO and the mass of the atmosphere is small. Diamond floats to an intermediate depth in the MO and thereby avoids segregation to the core. (C) Appreciable C is delivered to Earth by a late veneer of comets or icy planetesimals after crystallization of the MO.

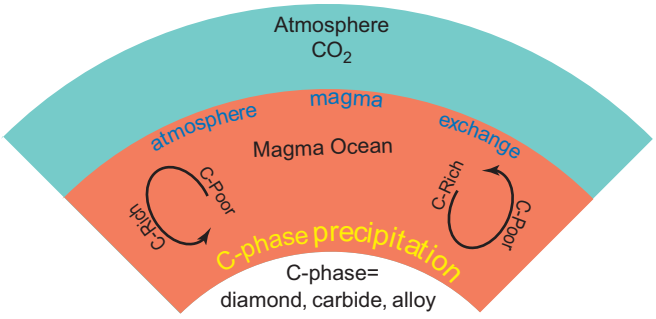

Fig. 8. Operation of a magma ocean carbon pump. Saturation deep in the MO with a C-rich phase depletes the magma in dissolved C. Mixing of this C-poor magma through the magma column reduces the dissolved C in the shallow MO, leading to dissolution of atmospheric C into the magma, which in turn is precipitated at the base of the MO. MO carbon pumps deposit large amounts of C as solids in the MO and buffer the magmatic and atmospheric C at low concentrations.

magma. The inventory of C–O–H volatiles in the resulting super-atmosphere depends on the processing on Earth prior to the giant impact, their concentrations and distribution in the embryo, and the magnitude of loss to space. Some have assumed that the post-giant impact atmosphere has a high CO_2 partial pressure (e.g., ~10 MPa; Zahnle et al., 2007), but C sequestration in the cores of both preexisting bodies, combined with loss owing to the impact (Genda and Abe, 2005), could produce a CO_2-poor atmosphere. Similarly, the initial redox state is uncertain, but interactions with the MO cannot allow it to be more reduced than that coexisting with the Fe^{3+}/Fe^{T} ratio defined by metal saturation at depth, and so H_2O and CO_2 probably dominated.

On cooling, equilibrium is approached by volatiles dissolving into the magma. Thus, the concentrations of magmatic volatiles are those imposed by the atmospheric vapor pressure. As volatiles are mixed down into the deeper portions of the MO and become more reduced, a C-rich phase may saturate. This sets up the conditions of a carbon pump (Fig. 8), drawing down the high concentrations of CO_2 in the atmosphere and storing much of the available carbon in the precipitating mantle.

6. Discussion

6.1. Iron disproportionation in magma oceans and the origin of Earth's oxidized mantle.

Earth's upper mantle is more oxidized than plausible saturation with Fe-metal. This may be due to disproportionation of Fe^{2+} in the lower mantle, yielding Fe and Fe^{3+} in Mg-perovskite (Wood and Halliday, 2005; Wood et al., 2006; Frost et al., 2008). In this scenario, small amounts of metal are produced in the solidified lower mantle and then removed by the later stages of core formation, either owing to renewed lower mantle melting associated with giant impacts, or entrainment by metal percolating downwards towards the core.

Deep MOs may disproportionate Fe^{2+} to Fe^{3+} and metal without requiring Mg-perovskite precipitation and removal of Fe from a solidified lower mantle. The iron in the silicate accreted to Earth consisted almost entirely of Fe^{2+}, owing to equilibration with metal at low pressure. According to the arguments in Section 3, once pressurized in a deep magma ocean, the Fe^{3+}/Fe^{T} ratio of the magma in equilibrium with metal might increase by a disproportionation reaction:

$$3\,Fe^{2+}_{magma} \Leftrightarrow 2\,Fe^{3+}_{magma} + Fe_{alloy}. \quad (3)$$

At the mean pressure of magma/metal equilibration (25–60 GPa), this reaction may produce an Fe^{3+}/Fe^{T} ratio similar to the present-day upper mantle value (~0.03–0.045; Canil et al., 1994; Cottrell and Kelley, 2011). Thus, the same magma may be in equilibrium with metal at high pressure and capable of crystallizing to a solid mantle that, in its shallow portions, is significantly more oxidized. A magma with Fe^{3+}/Fe^{T} of 0.03–0.045 is

sufficient to generate an overlying atmosphere dominated by H_2O and CO_2 (Section 3).

Note that if C is dissolved as carbonate in the shallow reaches of a MO, but reduced to CH_4 at depth, the change in oxidation state can influence the redox profile of the MO column. For example, for a MO underlying an atmosphere with 100 MPa CO_2 pressure there will be 60 ppm CO_2 (Fig. 4). Conversion of this to CH_4 at depth will change the Fe^{3+}/Fe^{T} of a magma with 8 wt% FeO^{T} by 0.005. This is a modest but not inconsequential effect compared to the range and uncertainty of upper mantle Fe^{3+}/Fe^{T} ratios (0.03–0.045). Additional effects may be related to reduction of dissolved H_2O to H_2, but more data on the solubility of H_2 at depth are needed.

6.2. A possible connection between early atmospheres and planetary size

Differences in redox conditions for MOs of planets of different sizes may influence the compositions of overlying atmospheres. If deep MOs produce oxidizing atmospheres and shallow MOs reducing ones, then Mars or Mercury may have had early atmospheres rich in CH_4 and H_2, whereas Earth and Venus may yield protoatmospheres rich in CO_2 and H_2O. This may set terrestrial planets on different evolutionary paths, with differences for the preservation potential of the atmospheres, the evolution of their climate, and development of conditions conducive to prebiotic chemistry.

6.3. The core could take all the carbon

Owing to the very high solubility of C in molten Fe alloy compared to silicate melts, virtually all of the C accreted to Earth could be dissolved in the core, leaving a nearly C-free mantle and exosphere. This could be true even if a MO equilibrated with only a fraction of a percent metal (Fig. 4). Further, if a modest amount of metal (~5%) equilibrated with the molten mantle, then a C-poor BSE could result even if the total delivery of C to Earth was extreme. For example, if $D_C^{all/sil} = 10^5$, then metal equal to 5% of the mass of the mantle would extract virtually all of the carbon from a planet that is >2.5 wt% C, leaving a BSE (mantle plus exosphere) with less than ½ of the low extrema of the estimated modern mass ($0.2–1.3 \times 10^{21}$ kg; Dasgupta and Hirschmann, 2010). Yet, the BSE today is comparatively C-rich.

There are three potential explanations as to how significant masses of terrestrial carbon avoided core sequestration (Fig. 7):

(A) High solubility of reduced C species (CH_4, CO) facilitated modest values of $D_C^{all/sil}$ and allowed the MO to retain appreciable C whilst equilibrated with metal. Values of $D_C^{all/sil}$ as large as 2×10^4 allow retention of C equal to the low estimate of the modern BSE. Values closer to 10^3 approach the high modern BSE estimate. These would require solubility in the magma of ~35–350 ppm methane under conditions of metal saturation (Fig. 5B). Such dissolved methane concentrations are quite plausible (Mysen et al., 2009; Ardia et al., 2011; Kadik et al., 2011), but may require comparatively high f_{H_2}.

(B) Owing to a paucity of available metal, a substantial mass of C precipitated as diamond and thereby escaped removal to the core. If the total amount of metal is low, then diamond saturation is likely, even if $D_C^{all/sil}$ is large.

(C) Much of the BSE inventory of C was delivered as part of a late veneer that post-dated core formation (Morbidelli et al., 2000; Dauphas and Marty, 2002; Javoy, 2005). Given dynamical simulations that show significant arrival of planetesimals from beyond the snow line late in Earth's accretion (e.g., Raymond et al., 2007), some portion of Earth's volatiles must derive from late events. Whether the majority arrived late is less certain. Objections to a volatile-rich late veneer arise from inconsistences with observed siderophile and noble gas abundances, and Os and W isotope ratios (Drake and Righter, 2002; Brandon et al., 2005; Halliday, 2008; Marty, 2012), but not all these critiques apply if the late veneer consisted partly of comets (e.g., Dauphas et al., 2000; Javoy, 2005; Hartogh et al., 2011), icy planetesimals (Albarède, 2009; Marty, 2012), or planetesimal compositions not represented in present meteorite collections (Albarède, 2009). Marty (2012) argued that depletion of nitrogen on Earth relative to C and H is a result of retention in the core or mantle during early differentiation. Similarly, Wood et al. (2010) showed that the highly siderophile moderately volatile elements, Te, Se, and S, are depleted by about two orders of magnitude compared to non-siderophile elements if of similar volatility. This strongly implies that these elements were present during core formation, and Morbidelli et al. (2012) used this to support dynamical arguments that most H_2O (and by extension, C) was delivered during the last 30–40% of accretion rather than as a late veneer. But if the BSE C arrived chiefly in a late veneer, then massive accumulation of C in the mantle occurred later by subduction or other ingassing mechanism (Sleep and Zahnle, 2001; Hirschmann and Dasgupta, 2009).

6.4. H/C fractionation between the mantle and exosphere—the role of a magma ocean carbon pumps

Today the inventory of C in the mantle is comparable to or exceeds that in the exosphere (Dasgupta and Hirschmann, 2010). A key expression of the magnitude of the modern deep C reservoir is the H/C ratio of the mantle, which is markedly lower than that of the exosphere (Hirschmann and Dasgupta, 2009). Mantle/exosphere H/C fractionation means either that the mantle preferentially retained C early in Earth history, or that subsequent time-integrated ingassing of C has been much more efficient than of H_2O.

Following removal of metal to the core, crystallization of the MO was previously thought to expel virtually all the dissolved C dissolved in silicate, yielding a C-poor mantle (Kuramoto and Matsui, 1996; Elkins-Tanton, 2008). Owing to incorporation in nominally anhydrous minerals (Kawamoto et al., 1996), the proportion of H_2O in the crystallized mantle will be markedly greater. Thus, following MO crystallization, the H/C ratio of the mantle would be high and that of the exosphere correspondingly low and so MO processes could produce H/C fractionations that are the opposite of conditions prevailing today.

Magma ocean carbon pumps (Sections 5.2 and 5.3) provide an alternative scenario, in which much of the BSE carbon could have precipitated during MO crystallization. Thus, the earliest mantle could have had a substantial C reservoir and a low H/C ratio. The mass of carbon pumped into the earliest solid mantle is potentially very large, but depends on the mass of C available to the MO and the saturation conditions of C-rich phases in the magma column. These in turn require improved constraints on the f_{O_2}-depth profile as well as the solubility of reduced C-species. The distribution of C in the mantle produced by C-pumping could be highly heterogeneous, with substantial C precipitated at restricted horizons. Presumably the C has since homogenized by convective mixing.

7. Conclusions

1. Well-mixed magma oceans with constant Fe^{3+}/Fe^{T} will have vertical zonation in f_{O_2}. At low pressure, f_{O_2} increases with depth, but this may reverse at high pressure. A deep MO

equilibrated with metal at depth may well have comparatively oxidized conditions at the surface and may be in equilibrium with an H_2O–CO_2 atmosphere.
2. Although small amounts of core-forming metal in a MO may absorb much of Earth's carbon, diamond saturation and floatation may retain significant concentrations in the mantle.
3. During MO crystallization, saturation in diamond or carbide can produce a C pump, depositing much of the C in the BSE in the mantle, rather than the atmosphere. This may account for the large inventory of C and low H/C ratio of the mantle.

Acknowledgments

I am grateful for the hospitality of colleagues at the Research School of Earth Sciences, ANU, where this manuscript was prepared during sabbatical leave. The paper was improved by the comments of Bernard Marty and two anonymous referees. This work was supported by Grants from NASA (NNX11AG64G) and NSF (EAR1119295).

References

Abe, Y., Matsui, T., 1985. The formation of an impact-generated H_2O atmosphere and its implications for the early thermal history of the Earth. J. Geophys. Res. 90, C545–C549.
Ahrens, T.J., O'Keefe, J.D., Lange, M.A., 1989. Formation of atmospheres during accretion of the terrestrial planets. In: Atreya, S.K., Pollack, J.B., Matthews, M.S. (Eds.), Origin and Evolution of Planetary and Satellite Atmospheres. University of Arizona Press, Tuscon, pp. 328–385.
Albarède, F., 2009. Volatile accretion history of the terrestrial planets and dynamic implications. Nature 461, 1227–1233.
Allwardt, J.R., Stebbins, J.F., Schmidt, B.C., Frost, D.J., Withers, A.C., Hirschmann, M.M., 2005. Aluminum coordination and the densification of high-pressure aluminosilicate glasses. Am. Mineral. 90, 1218–1222.
Archer, D., Eby, M., Brovkin, V., Ridgwell, A., Cao, L., Mikolajewicz, U., Caldeira, K., Matsumoto, K., Munhoven, G., Montenegro, A., Tokos, K., 2009. Atmospheric lifetime of fossil fuel CO_2. Annu. Rev. Earth Planet. Sci. 37, 117–134.
Ardia, P., Withers, A., Hirschmann, M., Hervig, R., 2011. 42nd Lunar and Planetary Science Conference, Abstract no. 1659.
Bada, J.L., 2004. How life began on Earth: a status report. Earth Planet. Sci. Lett. 226, 1–15.
Benz, W., Cameron, A.G.W., 1990. Terrestrial effects of the giant impact. In: Newsom, J.H., Jones, J.H. (Eds.), Origin of the Earth. Oxford University Press, Oxford, pp. 61–67.
Brandon, A.D., Humayun, M., Puchtel, I.S., Zolensky, M.E., 2005. Re–Os isotopic systematics and platinum group element composition of the Tagish Lake carbonaceious chondrite. Geochim. Cosmochim. Acta 69, 1619–1631.
Brearly, M., 1990. Ferric iron in silicate melts in the system Na_2O–Fe_2O_3–SiO_2 at high pressure. J. Geophys. Res. 95, 15703–15716.
Campbell, A.J., Danielson, L., Righter, K., Seagle, C.T., Wang, Y., Prakapenka, V.B., 2009. High pressure effects on the iron–iron oxide and nickel–nickel oxide oxygen fugacity buffers. Earth Planet. Sci. Lett. 286, 556–564.
Canil, D., O'Neill, H.S., Pearson, D.G., Rudnick, R.L., McDonough, W.F., Carswell, D.A., 1994. Ferric iron in peridotites and mantle oxidation-states. Earth Planet. Sci. Lett. 123, 205–220.
Canup, R.M., 2004. Simulations of a late lunar-forming impact. Icarus 168, 433–456.
Carroll, M.R., Stolper, E.M., 1993. Noble-gas solubilities in silicate melts and glasses—new experimental results for argon and the relationship between solubility and ionic porosity. Geochim. Cosmochim. Acta 57, 5039–5051.
Chabot, N.L., Draper, D.S., Agee, C.B., 2005. Conditions of core formation in the Earth: constraints from nickel and cobalt partitioning. Geochim. Cosmochim. Acta 69, 2141–2151.
Corgne, A., Keshav, S., Wood, B.J., McDonough, W.F., Fei, Y.W., 2008. Metal-silicate partitioning and constraints on core composition and oxygen fugacity during Earth accretion. Geochim. Cosmochim. Acta 72, 574–589.
Cottrell, E., Kelley, K.A., 2011. The oxidation state of Fe in MORB glasses and the oxygen fugacity of the upper mantle. Earth Planet. Sci. Lett. 305, 270–282.
Dahl, T.W., Stevenson, D.J., 2010. Turbulent mixing of meal and silicate during planet accretion—an interpretation of the Hf-W chronometer. Earth Planet. Sci. Lett. 295, 177–186.
Dasgupta, R., Hirschmann, M.M., 2010. The deep carbon cycle and melting in Earth's interior. Earth Planet. Sci. Lett. 298, 1–13.
Dasgupta, R., Walker, D., 2008. Carbon solubility in core melts in a shallow magma ocean environment and distribution of carbon between the Earth's core and the mantle. Geochim. Cosmochim. Acta 72, 4627–4641.
Davies, G., 1985. Heat deposition and retention in a solid planet growing by impacts. Icarus 63, 45–68.
Dauphas, N., Robert, F., Marty, B., 2000. The late asteroidal and cometary bombardment of Earth as recorded in water deuterium to protium ratio. Icarus 148, 508–512.
Dauphas, N., Marty, B., 2002. Inference on the nature and the mass of Earth's late veneer from noble metals and gases. J. Geophys. Res. 107 (art. no. 5129).
Day, H.W., 2012. A revised diamond–graphite transition curve. Am. Mineral. 97, 52–62.
Delano, J.W., 2001. Redox history of the Earth's interior since 3900 Ma: implications for prebiotic molecules. Origins Life Evol. Biosph. 31, 311–341.
Drake, M.J., Righter, K., 2002. Determining the composition of the Earth. Nature 416, 39–44.
Elkins-Tanton, L.T., 2008. Linked magma ocean solidification and atmospheric growth for Earth and Mars. Earth Planet. Sci. Lett. 271, 181–191.
Flaser, F.M., Birch, F., 1973. Energetics of core formation: a correction. J. Geophys. Res. 78, 6101–6103.
Fukai, Y., 1984. The iron–water reaction and the evolution of the Earth. Nature 308, 174–175.
Frost, D.J., McCammon, C.A., 2008. The redox state of Earth's mantle. Annu. Rev. Earth Planet. Sci. 36, 389–420.
Frost, D.J., Mann, U., Asahara, Y., Rubie, D.C., 2008. The redox state of the mantle during and just after core formation. Philos. Trans. R. Soc. A 366, 4315–4337.
Genda, H., Abe, Y., 2005. Enhanced atmospheric loss on protoplanets at the giant impact phase in the presence of oceans. Nature 433, 842–844.
Ghiorso, M.S., 2004. An equation of state for silicate melts. III. Analysis of stoichiometric liquids at elevated pressure: shock compression data, molecular dynamics simulations and mineral fusion curves. Am. J. Sci. 304, 752–810.
Ghiorso, M.S., Kress, V.C., 2004. An equation of state for silicate melts. II. Calibration of volumetric properties at 10^5 Pa. Am. J. Sci. 304, 679–751.
Halliday, A.N., 2008. A young Moon-forming giant impact at 70–110 million years accompanied by late-stage mixing, core formation and degassing of the Earth. Philos. Trans. R. Soc. A 366, 4163–4181.
Hartogh, P., Lis, D.C., Bockelee-Morvan, D., de Val-Borro, M., Biver, N., Kuppers, M., Emprechtinger, M., Bergin, E.A., Crovisier, J., Rengel, M., Moreno, R., Szutowicz, S., Blake, G.A., 2011. Ocean-like water in the Jupiter-family comet 103P/Hartley 2. Nature 478, 218–220.
Hashimoto, G.L., Abe, Y., Sugita, S., 2007. The chemical composition of the early terrestrial atmosphere: formation of a reducing atmosphere from CI-like material. J. Geophys. Res. 112, E0501.
Hirschmann, M.M., 2000. Mantle solidus: experimental constraints and the effects of peridotite composition. Geochem. Geophys. Geosyst. 1, 70.
Hirschmann, M.M., 2006. Water, melting, and the deep Earth H_2O cycle. Annu. Rev. Earth Planet. Sci. 34, 629–653.
Hirschmann, M.M., Withers, A.C., 2008. Ventilation of CO_2 from a reduced mantle and consequences for the early Martian greenhouse. Earth Planet. Sci. Lett. 270, 147–155.
Hirschmann, M.M., Dasgupta, R., 2009. The H/C ratios of Earth's near-surface and deep reservoirs, and consequences for deep Earth volatile cycles. Chem. Geol. 262, 4–16.
Hirschmann, M.M., Tenner, T.J., Aubaud, C., Withers, A.C., 2009. Dehydration melting of nominally anhydrous mantle: the primacy of partitioning. Phys. Earth Planet. Inter. 176, 54–68.
Höink, T., Schmalzl, J., Hansen, U., 2007. Dynamics of metal-silicate separation in a terrestrial magma ocean. Geochem. Geophys. Geosyst. 7, Q09008.
Hoffman, P.F., Kaufman, A.J., Halverson, G.P., Schrag, D.P., 1998. A Neoproterozoic snowball Earth. Science 281, 1342–1346.
Holloway, J.R., 1998. Graphite-melt equilibria during mantle melting: constraints on CO_2 in MORB magmas and the carbon content of the mantle. Chem. Geol. 147, 89–97.
Holloway, J.R., Pan, V., Gudmundsson, G., 1992. High-pressure fluid-absent melting experiments in the presence of graphite—oxygen fugacity, ferric ferrous ratio and dissolved CO_2. Eur. J. Mineral. 4, 105–114.
Huybers, P., Langmuir, C., 2009. Feedback between deglaciation, volcanism, and atmospheric CO_2. Earth Planet. Sci. Lett. 286, 479–491.
Ichikawa, H., Labrosse, S., Kurita, K., 2010. Direct numerical simulation of an iron rain in the magma ocean. J. Geophys. Res. 115, B01404.
Javoy, M., 2005. Where do the oceans come from? C. R. Geosci. 337, 139–158.
Kadik, A.A., Kurovskaya, N.A., Ignat'ev, Y.A., Kononkova, N.N., Koltashev, V.V., Plotnichenko, V.G., 2011. Influence of oxygen fugacity on the solubility of nitrogen, carbon, and hydrogen in FeO–Na_2O–SiO_2–Al_2O_3 melts in equilibrium with metallic iron at 1.5 GPa and 1400 degrees C. Geochem. Int. 49, 429–438.
Kawamoto, T., Hervig, R.L., Holloway, J.R., 1996. Experimental evidence for a hydrous transition zone of the early Earth's mantle. Earth Planet. Sci. Lett. 142, 587–592.
Kegler, P., Holzheid, A., Frost, D.J., Rubie, D.C., Dohmen, R., Palme, H., 2008. New Ni and Co metal-silicate partitioning data and their relevance for an early terrestrial magma ocean. Earth Planet. Sci. Lett. 268, 28–40.
Kress, V.C., 2004. Microsoft EXCEL spreadsheet-based program for calculating equilibrium gas speciation in the C–O–H–S–Cl–F system. Comput. Geosci. 30, 211–214.
Kress, V.C., Carmichael, I.S.E., 1991. The compressibility of silicate liquids containing Fe_2O_3 and the effect of composition, temperature, oxygen fugacity and pressure on their redox states. Contrib. Mineral. Petrol. 108, 82–92.
Kuramoto, K., Matsui, T., 1996. Partitioning of H and C between the mantle and core during the core formation in the Earth: its implications for the

atmospheric evolution and redox state of early mantle. J. Geophys. Res. 101, 14909–14932.
Lange, R.A., Carmichael, I.S.E., 1987. Densities of Na_2O–K_2O–CaO–MgO–FeO–Fe_2O_3–Al_2O_3–TiO_2–SiO_2 liquids—new measurements and derived partial molar properties. Geochim. Cosmochim. Acta 51, 2931–2946.
Li, J., Agee, C.B., 1996. Geochemistry of mantle–core differentiation at high pressure. Nature 381, 686–689.
Liu, Q., Lange, R.A., 2006. The partial molar volume of Fe_2O_3 in alkali silicate melts: evidence for an average Fe^{3+} coordination number near five. Am. Mineral. 91, 385–393.
Marty, B., 2012. The origins and concentrations of water, carbon, nitrogen, and noble gases on Earth. Earth Planet. Sci. Lett. 313, 56–66.
McCammon, C., 1997. Mg-perovskite as a possible sink for ferric iron in the lower mantle. Nature 387, 694–696.
Melosh, H.J., Vickery, A.M., 1989. Impact erosion of the primordial atmosphere of Mars. Nature 338, 487–489.
Miller, S.L., Urey, H.C., 1959. Organic compound synthesis on the primitive Earth. Science 130, 245–251.
Moore, G.M., Venneman, T., Carmichael, I.S.E., 1998. An empirical model for the solubility of water in magmas to 3 kilobars. Am. Mineral. 83, 36–42.
Morbidelli, A., Chambers, J., Lunine, J.I., Petit, J.M., Robert, F., Valsecchi, G.B., Cyr, K.E., 2000. Source regions and timescales for the delivery of water on Earth. Meteorit. Planet. Sci. 35, 1309–1320.
Morbidelli, A., Lunine, J.L., O'Brien, D.P., Raymond, S.N., Walsh, K.J., 2012. Building terrestrial planets. Annu. Rev. Earth Planet. Sci. 40, 251–275.
Mysen, B.O., Fogel, M.L., Morrill, P.L., Cody, G.D., 2009. Solution behavior of reduced C–O–H volatiles in silicate melts at high pressure and temperature. Geochim. Cosmochim. Acta 73, 1696–1710.
Mysen, B.O., Virgo, D., 1985. Iron-bearing silicate melts—relations between pressure and redox equilibria. Phys. Chem. Miner. 12, 191–200.
Nakajima, Y., Takahashi, E., Toshihiro, S., Funakoshi, K., 2009. "Carbon in the core" revisited. Phys. Earth Planet. Inter. 174, 202–211.
Okuchi, T., 1997. Hydrogen partitioning into molten iron at high pressure: implications for Earth's core. Science 278, 1781–1784.
O'Neill, H.S.C., 1988. Systems Fe–O and Cu–O: thermodynamic data for the equilibria Fe–"FeO", Fe–Fe_3O_4, "FeO"–Fe_3O_4 Fe_3O_4–Fe_2O_3, Cu–Cu_2O and Cu_2O–CuO from EMF measurements. Am. Mineral. 73, 470–486.
O'Neill, H.S.C., Berry, A.J., McCammon, C.C., Jayasuriya, K.D., Campbell, S.J., Foran, G., 2006. An experimental determination of the effect of pressure on the $Fe^{3+}/\sum$Fe ratio of an anhydrous silicate melt to 3.0 GPa. Am. Mineral. 91, 404–412.
O'Neill, H.S.C., McCammon, C.A., Canil, D., Rubie, D.C., Ross, C.R., Seifert, F., 1993. Mössbauer-spectroscopy of mantle transition zone phases and determination of minimum Fe^{3+} content. Am. Mineral. 78, 456–460.
Pan, V., Holloway, J.R., Hervig, R.L., 1991. The pressure and temperature-dependence of carbon-dioxide solubility in tholeiitic basalt melts. Geochim. Cosmochim. Acta 55, 1587–1595.
Pepin, R.O., 1991. On the origin and early evolution of terrestrial planet atmospheres and meteoritic volatiles. Icarus 92, 2–79.
Raymond, S.N., Quinn, T., Lunine, J.I., 2007. High-resolution simulations of the final assembly of Earth-like planets 2: water delivery and planetary habitability. Astrobiology 7, 66–84.
Rubey, W.W., 1951. Geologic history of sea water. Geol. Soc. Am. Bull. 62, 1111–1148.
Rubie, D.C., Melosh, H.J., Reid, J.E., Liebske, C., Righter, K., 2003. Mechanisms of metal-silicate equilibration in the terrestrial magma ocean. Earth Planet. Sci. Lett. 205, 239–255.
Schaefer, L., Fegley, B., 2007. Outgassing of ordinary chondritic material and some of its implications for the chemistry of asteroids, planets, and satellites. Icarus 186, 462–483.
Sleep, N.H., Zahnle, K., 2001. Carbon dioxide cycling and implications for climate on ancient earth. J. Geophys. Res. 106, 1373–1399.
Solomatov, V.S., 2000. Fluid dynamics of a terrestrial magma ocean. In: Canup, R., Righter, K. (Eds.), Origin of the Earth and Moon. University of Arizona Press, Tuscon, pp. 323–328.
Stevenson, D.J., 1990. Fluid dynamics of core formation. In: Newson, H.E., Jones, J. (Eds.), Origin of the Earth. Oxford University of Press, Oxford, pp. 231–249.
Stixrude, L., Karki, B., 2005. Structure and freezing of $MgSiO_3$ liquid in Earth's lower mantle. Science 310, 297–299.
Stixrude, L., de Koker, N., Sun, N., Mookherjee, M., Karki, B.B., 2009. Thermodynamics of silicate liquids in the deep Earth. Earth Planet. Sci. Lett. 226, 226–232.
Stribling, R.S.L.Miller, 1987. Energy yields for hydrogen cyanide and formaldehyde syntheses: the HCN and amino acid concentrations in the primitive ocean. Origins Life Evol. Biosph. 17, 261–273.
Suzuki, A., Ohtani, E., Kato, T., 1995. Flotation of diamond in mantle melt at high pressure. Science 269, 216–218.
Trail, D., Watson, E.B., Tailby, N.T., 2011. The oxidation state of Hadean magmas and implications for early Earth's atmosphere. Nature 480, 79–82.
Wood, B.J., Halliday, A.N., 2005. Cooling of the Earth and core formation after the giant impact. Nature 437, 1346–1349.
Wood, B.J., Walter, M.J., Wade, J., 2006. Accretion of the Earth and segregation of its core. Nature 441, 825–833.
Wood, B.J., Halliday, A.N., Rehkamper, M., 2010. Volatile accretion history of the Earth. Nature 467, E6–7.
Zahnle, K., Arndt, N., Cockell, C., Halliday, A., Nisbet, E., Selsis, F., Sleep, N.H., 2007. Emergence of a habitable planet. Space Sci. Rev. 129, 35–78.
Zhimulev, E.I., Chepurov, A.I., Sinyakova, E.F., Sonin, V.M., Cheperov, A.A., Pokhilenko, N.P., 2012. Diamond crystallization in the Fe–Co–S–C and Fe–Ni–S–C systems and the role of sulfide-metal melts in the genesis of diamond. Geochem. Int. 50, 205–216.
Ziethe, R., 2009. Settling of metal droplets in a terrestrial magma ocean: on the correction of the Stokes velocity. Planet. Space Sci. 57, 306–317.